

Hemicylindrical and toroidal liquid microlens formed by pyro-electro-wetting

Lisa Miccio,^{1,*} Melania Paturzo,¹ Simonetta Grilli,¹ Veronica Vespini,¹ and Pietro Ferraro^{1,2}

¹Istituto Nazionale di Ottica Applicata (CNR-INOA) Via Campi Flegrei 34, 80078 Pozzuoli (NA), Italy

²E-mail: pietro.ferraro@inoa.it

*Corresponding author: lisa.miccio@inoa.it

Received January 16, 2009; revised February 18, 2009; accepted February 19, 2009;
posted March 4, 2009 (Doc. ID 106465); published March 26, 2009

We found that by opportune functionalization of a polar dielectric substrate, a self-arrangement of hemicylindrical or toroidal-shaped liquid droplets can be obtained. The process takes place when a thermal stimulus is provided to a poled substrate whose surface is covered by an oily substance layer. Liquid droplet self-arrangement is due to the pyroelectric effect, and interferometric characterization of the droplets is also reported. We investigated this open microfluidic system for exploring the possibility to obtain liquid cylindrical microlens with variable focal length. Liquid microtoroidal structures arrays are also realized. They could find application as resonant liquid microcavities for whispering gallery modes. © 2009 Optical Society of America

OCIS codes: 010.1080, 230.3990, 090.1995, 160.3730.

Microlenses have a significant impact on microtechnologies in many fields ranging from microelectronics to optical communications and biotechnology. Various approaches were investigated to fabricate either single microlenses or arrays made with different materials [1–5]. The possibility to change the focal length by thermal actuation was demonstrated with polydimethylsiloxane (PDMS) [6] and SU8 [7] polymeric single microlenses. Among the different classes of microlenses, lenses made with liquids have the main advantage that they can be easily tuned [1,2,4,8–10]. Using liquid crystals, the focus tunability was obtained by changing the index of refraction through the application of an electric voltage [11]. Conversely, in liquid microlenses based on hydrostatic pressure, a deformable membrane allows one to change the focal power [2]. One valuable method to actuate liquid is based on electro-wetting (EW). By EW [12] lenses and other optofluidic components such as prisms, arrays elements for display, optical switches [13], and also a tunable fluidic axicon [14] have been realized. Recently a novel concept in EW was demonstrated and named pyro-electro-wetting (PEW), in which a polar dielectric substrate, exhibiting pyroelectric properties, is used to generate liquid microlens arrays. Arrays made of thousands of 100 μm diameter spherical lenses are obtained with the PEW approach. Such an array of liquid microlenses also exhibits a focal power tunability during temperature changes [15,16].

Even if many approaches have been found to realize liquid lenses, to the best of our knowledge, there have been only a few cases of attempts to obtain cylindrical or toroidal lenses [17–19] investigated. Moreover, recently liquid droplets having hemicylindrical shape were obtained by inducing strong anisotropic wetting on nanopatterned surfaces [20].

Here we show how, by the PEW method and the opportune functionalization of a lithium niobate (LN) substrate, it is possible to induce spontaneous formation of hemicylindrical or even hemitoroidal liquid

structures. Moreover, an accurate interferometric characterization of a cylindrical liquid structure is performed during the formation process. Furthermore we show that an array of liquid hemitoroidal lenses can be obtained on microscale dimensions that could find application as resonant microcavities for whispering gallery modes [21,22].

In the PEW approach, the pyroelectric property of a z -cut periodically poled LN (PPLN) wafer is used [23,24]. The poling process consists of spontaneous polarization inversion. A periodically poled crystal is a sequence of regions where the direction of polarization is alternately inverted. The periodicity and configuration of different domains are obtained by electric poling. Here, different from the previous work [15,16], we investigate two different types of lenses: cylindrical and toroidal. The crystal is covered by a thin film of an oily substance, and then it is heated and cooled in order to modify the shape of the liquid matter. During the temperature change we observed fast reshaping of the oil. In the cylindrical case, the process tends to an equilibrium state where the oil is gathered up in stripes along ferroelectric domain boundaries. These stripes exhibit lensing behavior, and we characterize their focal length by means of a digital holographic (DH) microscope [24]. In the literature many authors have measured the focal length variations of liquid lenses by indirect calculations. Indeed, they calculated the height of the lens and then recovered the focal length or measured the focal spot formation [1,2,4,7,8]. We performed an interferometric DH analysis that allows a direct measurement of the focal length from the computed complex wavefront at the exit pupil of the lens. A cylindrical and a toroidal liquid lens are formed by means of diverse poling geometries. In both cases a substrate of 500- μm -thick z -cut LN crystal with both sides polished is used. A mask lithography process is performed to generate the resist pattern corresponding to the expected geometry. Then high voltage is applied to reverse the domains by means of standard

electric field poling. To produce the cylindrical lens a linear geometry of periodically poled domain is fabricated. On the contrary, to form toroidal lenses, either a single large domain with circular geometry or an array of hexagonal domains was generated in the LN crystal. Optical microscope images of the samples are shown in Fig. 1. For the PPLN sample [Fig. 1(a)] the poled region has a period of $19\ \mu\text{m}$ and is about 1 mm wide, while the reverse domain polarity on the crystal surface is sketched in Fig. 2(a).

The samples are covered by a liquid substance, pentanoic acid, which belongs to the group of fatty acids and appears as an oily liquid. The liquid is spread on the PPLN substrate by means of a spin coater with a rate of 3000 rpm so that the liquid film has a uniform thickness of about $100\ \mu\text{m}$. The sample is positioned on a thermocontrolled hot plate, and the liquid movements on the substrate are recorded while the temperature is changing. The liquid topography variation during the heating and cooling processes while the temperature ranges from 30°C to 100°C is first observed by an optical microscope in reflection mode. Further details on the experimental procedure can be found in a previous paper from the same authors [15].

The thermocontrolled plate is made of a Peltier cell driven by a software. An NTC sensor measures the temperature of the sample. The device is able to furnish temperature ramps and cycles. The reported results are obtained heating and cooling the sample by means of controlled ramps. We observed that during the cooling process the covering substance modifies its shape in a regular and repeatable way. In the final oil distribution, shown in Fig. 2(b), two cylindrical profiles appear with their principal axis normal to the walls of the periodic domain pattern. As described in the sketch of Fig. 2(c), the presence of an electric surface charge, generated by the pyroelectric effect, lowers the surface tension owing to the repulsion between like charges [12]. Therefore the liquid matter is accumulated at the boundary of the domains in order to minimize the energy of the whole system. The details of the physics are outside the scope of this Letter and can be found in [12,16]. It is important to note that, as shown in Fig. 2(b), the fine PPLN structure does not affect the final overall behavior of the liquid that is collected along the main domains walls as for the case shown in Fig. 2(d), where only two domain walls exist. In Fig. 2(d) the toroidal lens is shown. For this configuration the re-

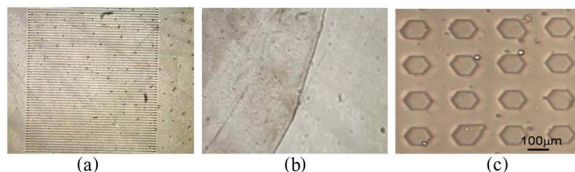


Fig. 1. (Color online) (a) Image of the PPLN sample used for the cylindrical lens. (b) Image of a part of the domain wall used for single toroidal lens. (c) Typical periodic hexagonal structures used to form a microarray of toroidal lenses. Due to the strong refractive index variation along the domain walls, these are clearly visible with an optical microscope.

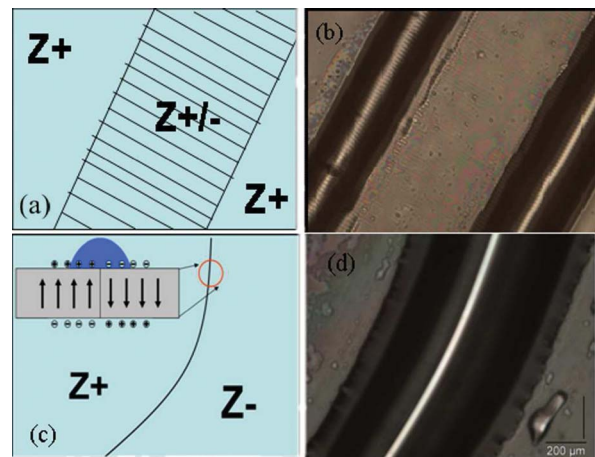


Fig. 2. (Color online) Schematic pictures of the poled region for (a) the PPLN sample and (c) the single domain wall. Optical microscope image of [(b), Media 1] cylindrical liquid lens and (d) toroidal lens.

verse domain has a diameter of 5 mm and a circular geometry. During the cooling process the covering substance collects itself along the domain wall, disappearing in the reversed and unreversed regions.

In Fig. 3(a) a configuration of a PPLN sample with a two-dimensional geometry is shown. The oil is collected again along the domain borderline of each hexagon. It is possible to observe that liquid follows the geometry of the hexagonal poled structures even in the region where this geometry is not regular. These microarrays of liquid toroidal structures can find application as resonant liquid microcavities [21,22]. To characterize the liquid lenses *in situ*, we adopted a DH interferometer in transmission configuration. The sample was put on a hotplate and positioned in a DH setup. By DH we performed an interferometric analysis to quantify the focal length for the liquid lens during its formation process. The setup is based on a Mach-Zehnder interferometer with a laser emitting at 532 nm [Fig. 3(b)]. The object wave passes through the sample; then it is collected by a microscope objective and made to interfere with the reference beam on a CCD camera placed at distance d from the image plane (named the reconstruction distance). The complex wavefield in the image plane is numerically calculated, starting from the interference pattern recorded by the CCD, through the scalar theory of diffraction [24] and allows us to recover both the intensity distribution and the phase retardation. We recorded 100 holograms during the

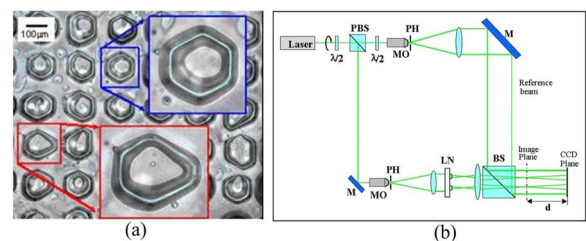


Fig. 3. (Color online) Liquid microarray of liquid toroidal structures. The liquid follows the nonuniform geometry of each hexagon. (b) DH setup based on a Mach-Zehnder interferometer

cooling process when the covering substance modifies itself to reach the final configuration shown in Fig. 2(b). The hologram recording rate is 15 frames/s, and the temperature is changed between 100°C and 30°C. We computed the complex wavefield for each hologram in the image plane of the cylindrical lens exit pupil. We calculated, for each hologram, the wrapped phase of the optical wavefront (i.e., the phase bonded between $-\pi$ and $+\pi$). We performed a numerical unwrapping procedure to recover the actual optical phase map. The wrapped and unwrapped phase maps, corresponding to the final frame, are shown in Figs. 4(a) and 4(b), respectively. Two movies showing the temporal evolution of the phase map at the exit pupil face are also available.

We performed a two-dimensional fitting procedure to evaluate the focal length of the cylindrical lens. The equation used is $\Delta\varphi = ax^2 + bxy + c$ [25]. From the coefficient of the quadratic term we calculate the focal length f according to the equation: $a = \pi/\lambda f$. The focal length varies from infinity to a very short value. The final focal length is $f = (690 \pm 20) \mu\text{m}$. The fitted surface obtained is shown in Fig. 4(a), while the experimental data and fitting results for a cylindrical lens cross section are reported in Fig. 4(b).

In conclusion, we found a method to form liquid droplets having a semitoroidal and cylindrical shape by a new type of EW, where neither electrodes nor an electrical power supply are necessary. The method, which we have named PEW, allows self-formation of special liquid droplets by functionalizing a polar dielectric crystal (actually a z -cut LN crystal). The focal length variation goes from infinity (when the liquid layer is flat before the thermal stimulus is applied) up to a final value $f = 690 \mu\text{m}$ when a stable configuration is reached. Such liquid droplets can be used as liquid cylindrical lenses that are suitable in many field of optics where focusing light along one direction is required. This allows us to induce and/or correct

anamorphism in laser beam and images, recover astigmatism in images, focus light into a slit, or converge light onto a line scan detector. Also a liquid microarray of toroidal lenses has been demonstrated. Further investigation will be devoted to accomplishing tuning by changing the temperature over a reduced range of temperatures even after lens formation.

References

1. S. Kuiper and B. H. W. Hendriks, *Appl. Phys. Lett.* **85**, 1128 (2004).
2. N. Chronis, G. L. Liu, K.-H. Jeong, and L. P. Lee, *Opt. Express* **11**, 2370 (2003).
3. P.-H. Huang, T. C. Huang, Y.-T. Sun, and S. Y. Yang, *Opt. Express* **16**, 3041 (2008).
4. H. Ren and S.-T. Wu, *Opt. Express* **16**, 2646 (2008).
5. L. Pang U. Levy, K. Campbell, A. Groisman, and Y. Fainman, *Opt. Express* **13**, 9003 (2005).
6. S. Y. Lee, H. W. Tung, W. C. Chen, and W. Fang, *IEEE Photon. Technol. Lett.* **18**, 2191 (2006).
7. X. Huang, C. M. Cheng, L. Wang, C. C. Su, M. S. Ho, P. R. LeDuc, and Q. Lin, *Appl. Phys. Lett.* **92**, 251904 (2008).
8. P. M. Moran, S. Dharmatilleke, A. H. Khaw, K. W. Tan, M. L. Chan, and I. Rodriguez, *Appl. Phys. Lett.* **88**, 041120 (2006).
9. B. Berge and J. Peseux, *Eur. Phys. J. E* **3**, 159 (2000).
10. C. C. Cheng and J. A. Yeh, *Opt. Express* **15**, 7140 (2007).
11. L. G. Commander, S. E. Day, and D. R. Selviah, *Opt. Commun.* **177**, 157 (2000).
12. L. Lin Jr., G. B. Lee, Y. H. Chang, and K. Y. Lien, *Langmuir* **22**, 484 (2006).
13. J. Heikenfeld, N. Smith, M. Dhindsa, K. Zhou, M. Kilaru, L. Hou, J. Zhang, E. Kreit, and B. Raj, *Opt. Photonics News* **20**(1), 20 (2009).
14. G. Milne, G. D. M. Jeffries, and D. T. Chiu, *Appl. Phys. Lett.* **92**, 261101 (2008).
15. P. Ferraro, L. Miccio, S. Grilli, A. Finizio, S. De Nicola, and V. Vespini, *Opt. Photonics News* **19**(12), 34 (2008).
16. L. Miccio, A. Finizio, S. Grilli, V. Vespini, M. Paturzo, S. De Nicola, and P. Ferraro, *Opt. Express* **17**, 2487 (2009).
17. X. Mao, J. R. Waldeisen, B. K. Juluri, and T. J. Huang, *Lab Chip* **7**, 1303 (2007).
18. H. Ren, Y. H. Fan, S. Gauza, and S. T. Wu, *Jpn. J. Appl. Phys.* **44**, 243 (2005).
19. J. H. Lee, Y. H. Ho, K. Y. Chen, H. Y. Lin, J. H. Fang, S. C. Hsu, J. R. Lin, and M. K. Wei, *Opt. Express* **16**, 21184 (2008).
20. D. Xia and S. R. J. Brueck, *Nano Lett.* **8**, 2819 (2008).
21. A. Kiraz, Y. Karadag, and A. F. Coskun, *Appl. Phys. Lett.* **92**, 191104 (2008).
22. S. I. Shopova, H. Zhou, X. Fan, and P. Zhang, *Appl. Phys. Lett.* **90**, 221101 (2007).
23. S. Grilli, M. Paturzo, L. Miccio, and P. Ferraro, *Meas. Sci. Technol.* **19**, 074008 (2008).
24. P. Ferraro, S. Grilli, M. Paturzo, and S. Nicola, in *Ferroelectric Crystals for Photonic Applications*, P. Ferraro, S. Grilli, and P. De Natale, eds. (Springer, 2008), pp. 165–208.
25. D. Malacara and S. L. DeVore, in *Optical Shop Testing*, D. Malacara, ed. (Wiley, 1992), pp. 455–480.

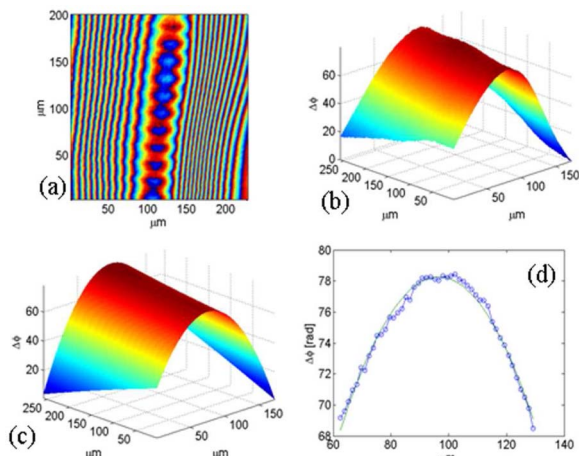


Fig. 4. (Color online) (a) Wrapped phase distribution (Media 2) and (b) unwrapped phase distribution of the optical wavefront of the final frame at 30° (Media 3). (c) Fitted surface obtained by the two-dimensional fitting procedure, (d) focal length measurement at the stationary condition.